BUILDING DETECTION FROM HIGH RESOLUTION DIGITAL ELEVATION MODELS IN URBAN AREAS

Michel JORDAN, Matthieu CORD, Thomas BELLI
ETIS - Equipe Image
UPRES-A CNRS 8051
ENSEA
6, avenue du Ponceau
F 95014 CERGY PONTOISE CEDEX - FRANCE
{jordan, cord, belli}@ensea.fr

KEY WORDS: DEM, DTM, frequency model estimation, building detection.

ABSTRACT

This paper describes an algorithm which aims at deriving digital terrain models (DTM) from dense digital elevation models (DEM). This algorithm takes place in a processing chain for building detection and modelling in urban areas from high resolution aerial imagery. DEM either come from stereophotogrammetry, or from direct measures such as airborne laser data. DTM are computed as low order frequency models, which exclude "high frequencies" such as buildings and other man-made structures. Above-ground regions are then detected by differences between DEM and DTM. Our processing chain ends with the 3D building modelling.

1 INTRODUCTION

Automatic and semi-automatic extraction of cartographic objects is a very intensive research field; a lot of investigations concerns road and building detection and modelling (Grün et al., 1995, Grün et al., 1997, Baltsavias et al., 2001).

Many applications (urban planning, telecommunication antenna localization, ...) concern urban areas, which are characterized by dense information need, sharp relief discontinuities, large occlusion areas, numerous and various building sizes, shapes and appearances. An overview and classification of methods developed in order to deal with such data and characteristics can be found in (Mayer, 1999).

In this paper, we present an algorithm for deriving digital terrain models (DTM) from dense digital elevation models (DEM). This algorithm takes place in our processing chain for building detection and modelling from high resolution aerial image stereopairs (Cord et al., 2001). In section 2, we briefly remind our dense DEM computation algorithm, which provides data for DTM estimation; section 3 presents the DTM model and the estimation algorithm; we provides results on synthesis data, in a quality assessment purpose, as well as on some real data (section 4).

2 DEM COMPUTATION

We developed a specific algorithm for dense elevation map computation from high resolution aerial stereopairs (Cord et al., 1999). Such images in urban areas are characterized by large occlusion areas, large non or poor textured areas, large disparity intervals. Our algorithm relies on an adaptive window cross-correlation matching process, integrated in a multi-resolution coarse-to-fine approach, with symmetric validation at each level of the image pyramids. This algorithm, initially developed for greylevel stereopairs, has been extended to colour images (Belli et al., 2000).

As an example, figure 1 shows a dense DEM obtained with this algorithm, applied to an high resolution aerial stereopair (images from the IGN digital camera, resolution about 25cm per pixel, image size is 1700×1450).

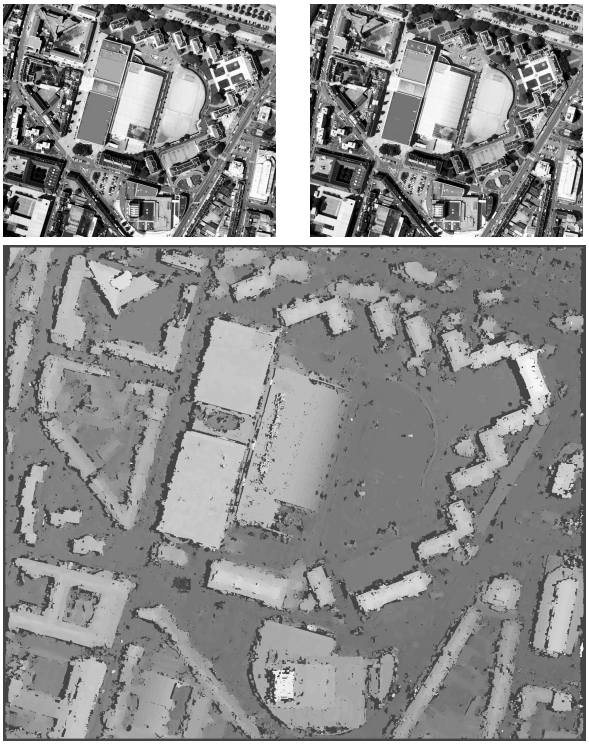

Figure 1: High resolution aerial stereopair and DEM computation: the DEM geometry is the left image's one, black pixels are non matched ones, and brighter greylevels correspond to higher elevations.

3 DTM FROM DEM COMPUTATION

3.1 DTM model

Our processing chain aims at detecting and modelling cartographic features such as buildings. After dense DEM

computation, the following step consists in the DTM estimation, which will then allow to detect above-ground regions (and especially buildings) from the differences between the DEM and the DTM. We presented a first version of our DTM estimation algorithm in (Belli et al., 2001).

The DTM is modelled as a decomposition of order N on a basis of 2D harmonic functions; the elevation field $z(x, y)$ is written as:

$$\begin{aligned} z(x,y) &= a_{0,0} \\ &+ \sum_{k,l=0\,;\,k+l\neq 0}^{N} a_{k,l}\cos(2\pi(k\nu_x x + l\nu_y y)) \\ &+ \sum_{k,l=0\,;\,k+l\neq 0}^{N} b_{k,l}\sin(2\pi(k\nu_x x + l\nu_y y)) \end{aligned} \quad (1)$$

where the fundamental frequencies $\nu_x = 1/T_x$ and $\nu_y = 1/T_y$ are computed from the DTM size $T_x \times T_y$. N is the model order, and it can be seen as a constraint on the terrain variability. Using such a model, the DEM points either belong to the DTM or are "outliers" for the DTM computation (above ground points, *i.e.* building or vegetation).

3.2 Robust estimation

We developed a robust statistical estimation algorithm in order to compute the $P = 2\cdot(N+1)^2-1$ model parameters from the m DEM points $[x_i, y_i, z(x_i, y_i)]_{i=1,m}$.

We build the following matrix equation:

$$z = M \cdot \Theta \quad (2)$$

with:

$$\Theta = [a_{0,0}, a_{0,1}, b_{0,1}, \ldots, a_{N,N}, b_{N,N}]^t$$

$$M = \begin{pmatrix} 1 & C_{0,1}(1) & S_{0,1}(1) & \ldots & S_{N,N}(1) \\ 1 & \vdots & \vdots & \vdots & \vdots \\ 1 & C_{0,1}(m) & S_{0,1}(m) & \ldots & S_{N,N}(m) \end{pmatrix}$$

where $C_{k,l}(i) = \cos(2\pi(k\nu_x x_i + l\nu_y y_i))$ and $S_{k,l}(i) = \sin(2\pi(k\nu_x x_i + l\nu_y y_i))$.

The resolution scheme of this over-determined ($m \gg P$) system is based on the M-estimators theory, which consists in iteratively reducing the influence of outliers (above-ground points). The optimal solution Θ_ρ computation involves the minimization of a function ρ of the error $\epsilon_\Theta(i)$ on axis Oz between data $z(x_i, y_i)$ and model $(M \cdot \Theta)(i)$:

$$\Theta_\rho = \arg\min_{\Theta} \sum_{i=1,m} \rho(\epsilon_\Theta(i)) \quad (3)$$

In a first version of our algorithm, we used the Tukey's norm as ρ function (c is a scale factor):

$$\rho_c(x) = \begin{cases} \frac{c^2}{6}(1-(1-(\frac{x}{c})^2)^3) & \text{if} \quad |x| \leq c \\ \frac{c^2}{6} & \text{otherwise} \end{cases}$$

The weight function w_c corresponding to this norm is:

$$w_c(x) = \begin{cases} (1-(\frac{x}{c})^2)^2 & \text{if} \quad |x| \leq c \\ 0 & \text{otherwise} \end{cases}$$

The numerical resolution scheme lies on the solution of the matrix form of the iterated equation (for iteration k) until convergence:

$$\hat{\Theta}^{(k)} = (M^t\, W_c^{(k)}\, M)^{-1}\, M^t\, W_c^{(k)}\, z \quad (4)$$

with $W_c^{(k)} = diag(w_c(\epsilon_\Theta^{(k-1)}))$ the diagonal weight matrix.

However, our problem is not a symmetric one; on the opposite, we could consider that all DEM points which have a negative error $\epsilon_\Theta^{(k-1)}$ are likely to be ground points. So we developed a resolution scheme based on an "asymmetric Tukey's norm" and the associated weight function:

$$w_c(x) = \begin{cases} 1 & \text{if} \quad x \leq 0 \\ (1-(\frac{x}{c})^2)^2 & \text{if} \quad 0 < x \leq c \\ 0 & \text{otherwise} \end{cases}$$

In the following section, we present results obtained with this model from synthesis data in various ground and above-ground configurations.

4 RESULTS ON SYNTHESIS DATA

4.1 Synthesis data

The first element of our synthesis data is a synthesis DTM $z(x, y) = \sum_{k,l=0}^{N} a_{k,l}\cos(2\pi(k\nu_x x + l\nu_y y))$ where the coefficients $a_{k,l}$ are randomly chosen (fig. 2, left).

We add on this DTM a certain number of "flat roof buildings" (fig. 2, right, example with 6 "buildings"), and finally some Gaussian noise modelling stereo-matching errors.

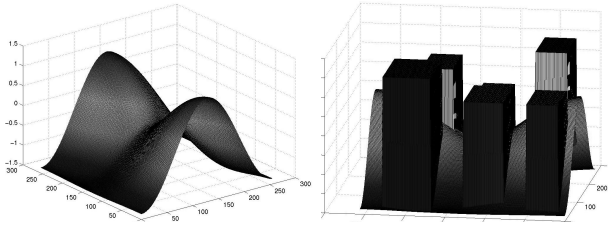

Figure 2: Synthesis DTM (left) and DEM (right).

The parameters of our synthesis DEM are then:

- the order N and the coefficients of the DTM;
- the number of buildings and their sizes (width, length and height);
- the Gaussian noise standard deviation σ.

We tested our DTM estimator on various configurations of buildings (number, heights, and ratio between ground and above-ground points), and with different values of σ. We have also assessed the influence of the Tukey's norm scale factor c.

4.2 Evaluation

In the following paragraphes, we present some assessments of our algorithm with these synthesis data. In order to do easiest comparisons, we generally present some DEM and DTM line and/or column profiles ; along these profiles, the reference DTM is light blue, the DEM is dark blue and the DTM estimation is red.

Tukey's scale factor c: this factor controls the weighting of DEM points for the DTM estimation: the bigger c, the bigger $w_c(x)$, and the less selective our estimator. The estimation strategy consists in starting with a few selective estimator (with a great value of c), and we progressively select less and less points, by decreasing the c value. We found experimentally — and thus confirm our initial intuition — that the value of c_{min} should be about the height of the lowest above-ground structure that we want to reject from the DTM. It makes no sense for c_{max} to be greater than the DEM height amplitude, and we used experimentally about 20 values of c from c_{max} to c_{min}.

Gaussian noise standard deviation: we added Gaussian noise with standard deviation σ between $0.$ and 2.5 (the DTM height amplitude of our synthesis data is about $3.$ units and the "building" heights between 0.5 and 1.3 units). The curves on figure 3 shows the mean quadratic error of DTM estimation (*i.e.* the difference between reference DTM and estimation) for several estimators (different values of N, weight functions are either the original Tukey's norm or the asymmetric one).

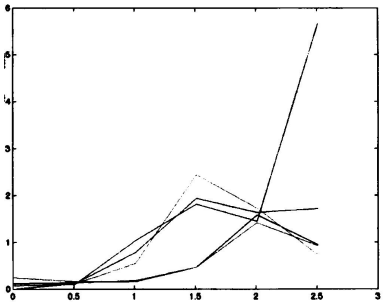

Figure 3: Mean quadratic error of DTM estimation against Gaussian noise standard deviation, for several estimation modes and strategies.

This figure does not allow us to make difference between estimators against the Gaussian noise, provided that the value of σ is less than the building heights... For greater values of σ, performances decrease fast (curves for $\sigma \geq 2.$ have no real signification, because this noise amplitude does not allow to distinguish between "terrain" and "buildings").

Height of buildings: we tested various ratios between building heights, DTM amplitude and Gaussian noise standard deviation. Figure 4 shows line and column profiles for small values of building height (building height and DTM amplitude have about the same value); figure 5 shows profiles for another configuration, where buildings have very different heights from each other.

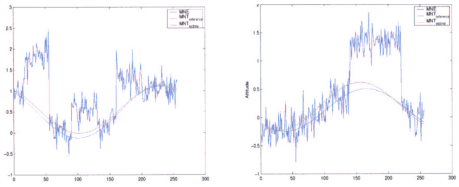

Figure 4: Line and column profiles for low buildings.

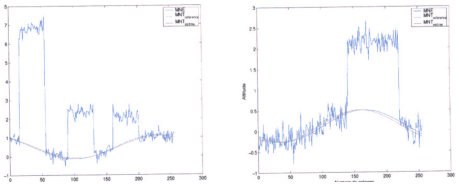

Figure 5: Line and column profiles for buildings having different heights.

Both cases — and the other ones which are not presented here — show that the DTM estimation quite well fits the reference DTM.

Number of buildings: we added 3, 6 and 10 buildings on our reference DTM (figures 6 and 7 for 3 and 10 buildings respectively). For all these configurations, the mean accuracy is about $5 \cdot 10^{-2}$. The number of buildings, and the ratio between ground and above-ground points (under the limit of 50%, the terrain model makes less sense) does not seem to be a critical parameter.

4.3 Results on real data

We used our algorithm to compute DTM from real images from the IGN digital camera. Figure 8 shows such a DTM; the reference color image is presented on the left; on the DEM shown at center of the figure, altitudes grow from dark blue to red, and one clearly perceive the terrain slope in the North-South direction. The 3D perspective view of the DEM (left of the figure) makes the terrain slope more clearly visible.

5 CONCLUSION

We have presented here an improved version of our algorithm for DTM estimation from dense DEM. This algorithm is based on a DTM model as a sum of harmonic functions, and robust M-estimators are used to iteratively select ground points and compute the DTM model. It has been tested with synthesis data, and DTM estimation seems quite robust with very different DEM configurations. We have then successfully applied it to dense DEM computed from aerial stereo images matching in urban areas. However, our algorithm could also be applied to other data such as airborne laser DEM.

After this process, the difference between the DEM and the DTM provides a "relative DEM", which we are able to segment in order to extract above-ground objects (buildings and trees).

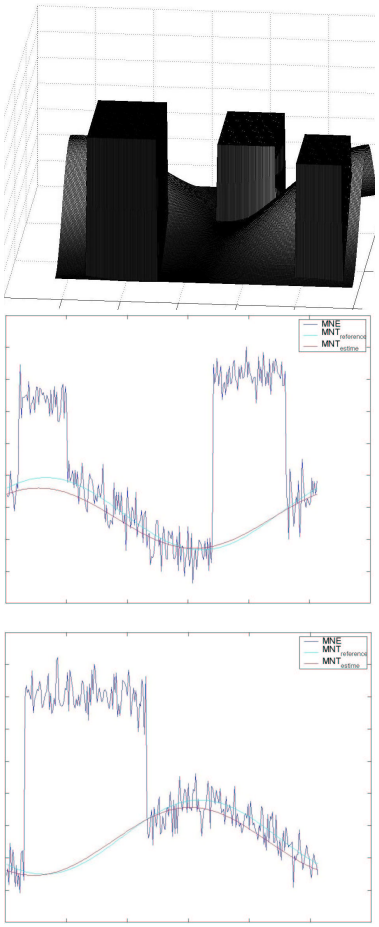

Figure 6: Assessment with 3 buildings: DEM (top), column 153 profile (center) and line 207 profile (bottom).

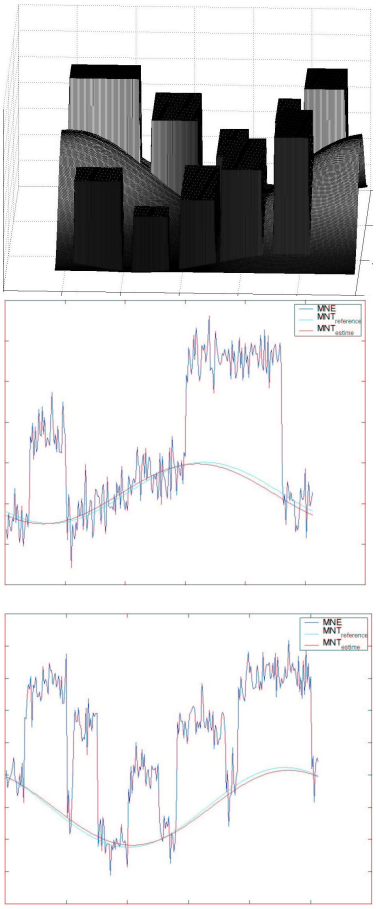

Figure 7: Assessment with 10 buildings: DEM (top), column 153 profile (center) and line 207 profile (bottom).

We particularly thank the french Institut Géographique National, which provided high resolution aerial images from its new digital camera.

REFERENCES

Baltsavias, E., Grün, A. and Van Gool, L. (eds), 2001. Automatic Extraction of Man-Made Objects from Aerial and Space Images (III). A.A. Balkema Publishers, Lisse.

Belli, T., Cord, M. and Jordan, M., 2001. 3D data reconstruction and modeling for urban scene analysis. In: 3rd Workshop on Automatic Extraction of Man-Made Objects from Aerial and Space Images, Ascona, Switzerland.

Belli, T., Cord, M. and Philipp-Foliguet, S., 2000. Colour Contribution for Stereo Image Matching. In: Proc. of Int. Conf. on Colour in Graphics and Image Processing, CGIP'2000, Saint-Etienne, France, pp. 317–322.

Cord, M., Jordan, M. and Cocquerez, J.-P., 2001. Accurate Building Structure Recovery from High Resolution Aerial Images. Computer Vision and Image Understanding 82(2), pp. 138–173.

Cord, M., Jordan, M., Cocquerez, J.-P. and Paparoditis, N., 1999. Automatic Extraction and Modelling of Urban Buildings from High Resolution Aerial Images. In: H. Ebner, W. Eckstein, C. Heipke and H. Mayer (eds), Automatic Extraction of GIS Objects from Digital Imagery, Vol. 32number 3-2W5, ISPRS, München, pp. 187–192.

Grün, A., Baltsavias, E. and Henricsson, O. (eds), 1997. Automatic Extraction of Man-Made Objects from Aerial and Space Images (II). Birkhäuser Verlag, Basel.

Grün, A., Kübler, O. and Aggouris, P. (eds), 1995. Automatic Extraction of Man-Made Objects from Aerial and Space Images. Birkhäuser Verlag, Basel.

Mayer, H., 1999. Automatic Object Extraction from Aerial Imagery — A Survey Focusing on Buildings. Computer Vision and Image Understanding 74(2), pp. 138–149.

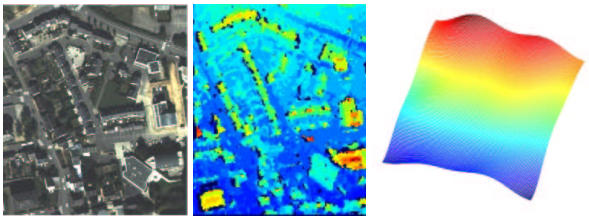

Figure 8: DTM estimation from aerial images: aerial reference image (left), DEM (center), and DTM 3D view (right).